



TITLE:

# Martian dust devil statistics from high-resolution large-eddy simulations

AUTHOR(S):

Nishizawa, Seiya; Odaka, Masatsugu; Takahashi, Yoshiyuki O.; Sugiyama, Ko-ichiro; Nakajima, Kensuke; Ishiwatari, Masaki; Takehiro, Shin-ichi; ... Sato, Yousuke; Tomita, Hirofumi; Hayashi, Yoshi-Yuki

---

CITATION:

Nishizawa, Seiya ...[et al]. Martian dust devil statistics from high-resolution large-eddy simulations. Geophysical Research Letters 2016, 43(9): 4180-4188

ISSUE DATE:

2016-05-16

URL:

<http://hdl.handle.net/2433/216117>

RIGHT:

© 2016. American Geophysical Union. All Rights Reserved.; 許諾条件により本文ファイルは2017-11-16に公開.

RESEARCH LETTER

10.1002/2016GL068896

Key Points:

- Quantitative considerations on statistics of Martian dust devils
- LES with 5 m resolution for 20 times 20 km<sup>2</sup> domain
- Frequency distributions of size, pressure drop, velocity, vorticity, and circulation of dust devils

Supporting Information:

- Supporting Information S1
- Figure S1

Correspondence to:

S. Nishizawa,  
[s-nishizawa@riken.jp](mailto:s-nishizawa@riken.jp)

Citation:

Nishizawa, S., et al. (2016), Martian dust devil statistics from high-resolution large-eddy simulations, *Geophys. Res. Lett.*, 43, 4180–4188, doi:10.1002/2016GL068896.

Received 12 NOV 2015

Accepted 14 APR 2016

Accepted article online 22 APR 2016

Published online 14 MAY 2016

## Martian dust devil statistics from high-resolution large-eddy simulations

Seiya Nishizawa<sup>1</sup>, Masatsugu Odaka<sup>2</sup>, Yoshiyuki O. Takahashi<sup>3</sup>, Ko-ichiro Sugiyama<sup>4</sup>, Kensuke Nakajima<sup>5</sup>, Masaki Ishiwatari<sup>2</sup>, Shin-ichi Takehiro<sup>6</sup>, Hisashi Yashiro<sup>1</sup>, Yousuke Sato<sup>1</sup>, Hirofumi Tomita<sup>1</sup>, and Yoshi-Yuki Hayashi<sup>3</sup>

<sup>1</sup>RIKEN Advanced Institute for Computational Science, Kobe, Japan, <sup>2</sup>Department of Cosmo sciences, Hokkaido University, Sapporo, Japan, <sup>3</sup>Department of Planetology/Center for Planetary Science, Kobe University, Kobe, Japan, <sup>4</sup>Department of Information Engineering, National Institute of Technology, Matsue College, Matsue, Japan, <sup>5</sup>Department of Earth and Planetary Sciences, Kyushu University, Fukuoka, Japan, <sup>6</sup>Research Institute for Mathematical Sciences, Kyoto University, Kyoto, Japan

**Abstract** Dust devils are one of the key elements in the Martian atmospheric circulation. In order to examine their statistics, we conducted high-resolution (up to 5 m) and wide-domain (about 20 × 20 km<sup>2</sup>) large-eddy simulations of the Martian daytime convective layer. Large numbers of dust devils developed spontaneously in the simulations, which enabled us to represent a quantitative consideration of Martian dust devil frequency distributions. We clarify the distributions of size and intensity, a topic of debate, and conclude that the maximum vertical vorticity of an individual dust devil has an exponential distribution, while the radius and circulation have power law distributions. A grid refinement experiment shows that the rate parameter of the vorticity distribution and the exponent of the circulation distribution are robust. The mode of the size distribution depends on the resolution, and it is suggested that the mode is less than 5 m.

### 1. Introduction

In the Martian atmosphere, dust has a significant effect on both general circulation and mesoscale storms. Accurately estimating the amount of dust injected from the surface into the atmosphere is important for understanding Martian atmospheric circulation. The injection mainly depends on surface winds [e.g., *Iversen and White*, 1982], which have mainly been investigated using laboratory experiments. Formally, in general circulation models (GCMs), dust lifting had simply been evaluated from surface wind stresses evaluated only by large-scale winds calculated explicitly using grid point quantities. However, it has been suggested that dust lifting by large-scale winds is not sufficient to maintain the average amount of dust in the Martian atmosphere [e.g., *Greeley et al.*, 1993; *Wilson and Hamilton*, 1996]; contributions from small-scale disturbances, especially dust devils, became recognized as important. The existence of dust devils on Mars was shown by *Thomas and Gierasch* [1985] and Mars Orbiter Camera observations by the Mars Global Surveyor [*Cantor et al.*, 2001]; in addition, other Martian explorations [e.g., *Lemmon et al.*, 2004], have revealed that dust devils are ubiquitous on Mars. *Rennó et al.* [1998] proposed a scaling theory for dust devils based on the heat engine framework of the planetary boundary layer (PBL), which calculates the potential mean intensity and occurrence of dust devils from ambient conditions. *Newman et al.* [2002] used this theory to estimate the amount of dust lifting by dust devils and developed a parameterization of dust lifting for GCMs. Through these works and other subsequent GCM studies, it has been recognized that dust devils are necessary to maintain the average amount of dust in the Martian atmosphere [e.g., *Rafkin et al.*, 2013].

Recently, the characteristics of Martian and terrestrial dust devils have been examined using observational data [e.g., *Lorenz*, 2011; *Fenton and Lorenz*, 2015]. These data suggest several possibilities for the distribution of dust devil size. However, the number of samples has not been statistically sufficient to clarify the distribution. Additionally, there may be an observational bias in detection efficiency that depends on dust devil size, and there are some dust devil characteristics that are difficult to represent using only observable quantities. Numerical studies of dust devils are needed to reduce the statistical uncertainty in such observational studies and to conduct further detailed analysis in order to understand the statistical characteristics of dust devils.

Numerical investigation of Martian dust devils began with studies of convection in the Martian PBL [e.g., *Odaka et al.*, 2001; *Rafkin et al.*, 2001]. Large-eddy simulations (LESs) showed that isolated vertical vortices are

spontaneously developed in the PBL during daytime [Toigo *et al.*, 2003; Michaels and Rafkin, 2004]. Numerous LES studies of the Martian PBL have been conducted [e.g., Petrosyan *et al.*, 2011]; however, they have been limited by the availability of computational resources. Therefore, most previous LES studies of Martian dust devils have focused on the structures of individual dust devils. Although the statistical characteristics of multiple dust devils have begun to be considered, mostly in terrestrial simulations [e.g., Ohno and Takemi, 2010; Gheynani and Taylor, 2011], the number of vortices is about 100 and is not enough for discussing the statistics of vortices with a wide variety of characteristics. Computational resources present a serious limitation in discussing the statistics of dust devils on Mars. The PBL on Earth is about 1 km in height, but the Martian PBL could be 10 km in height [e.g., Hinson *et al.*, 2008; Odaka, 2001], and convective cells in the PBL have a similar horizontal scale as the vertical scale of the PBL. Therefore, the domain size must be greater than 10 km in order to represent the convective cells of such a deep PBL and to render negligible the artificial influence of computational lateral boundaries on the cells. On the other hand, a resolution of tens of meters is necessary in order to represent all the vortices with size range of more than 1 order of magnitude (from tens to hundreds of meters).

In this study, we perform high-resolution and wide-domain LESs, through which we simulate a sufficient number of dust devils with a wide variety of horizontal sizes to clarify their frequency distributions. We examine the dependency of the obtained dust devil statistics on resolution using a grid refinement experiment with various spatial resolutions. The robustness of the results is considered based on the resolution dependency, which represents a quantitative description of the statistics of Martian dust devils.

## 2. Experimental Settings

We perform a Martian dust devil experiment using an LES model (SCALE-LES) [Nishizawa *et al.*, 2015; Sato *et al.*, 2015] with Martian atmospheric parameters. The domain size is a square measuring 19.2 km in the horizontal and about 21 km in the vertical. Double periodic conditions are adopted as lateral boundary conditions. The spatial resolution sweeps through grid spacings of 100, 50, 25, 10, and 5 m, and the same domain size is retained for each spacing. An isotropic grid is employed below 15 km, and the vertical grid spacing is gradually stretched with increasing height above this altitude.

The fully compressive equations are numerically solved with a fully explicit temporal integration scheme. Subgrid scale turbulence is parameterized by the Smagorinsky-type eddy viscosity model [Brown *et al.*, 1994; Scotti *et al.*, 1993]. Surface fluxes are calculated using the Louis-type model [Louis, 1979; Uno *et al.*, 1995]. Their details are described in Nishizawa *et al.* [2015]. External radiative heating calculated in the one-dimensional simulation conducted by Odaka *et al.* [2001] is used here instead of online calculations of the radiation process. The one-dimensional simulation is performed with the condition of  $L_s = 100^\circ$  at  $20^\circ\text{N}$ , where  $L_s$  is the areocentric longitude of the Sun, and the optical depth of dust is 0.2; the net shortwave flux at the surface is  $485 \text{ W m}^{-2}$  at noon. The surface temperature is also given externally from the one-dimensional simulation. Integrations are performed for one Martian day from the initial conditions of the horizontally uniform steady state at 00:00 local time (LT), except in the 5 m resolution run. The initial conditions include the vertical temperature profile obtained from the one-dimensional simulation and tiny random perturbations. For the 5 m run, integration is performed for 1 h from the state of the 10 m resolution run at 14:00 LT. Analyses are performed at 14:30 and 15:00 LT, at which time the PBL is almost at its deepest. The turbulence in the PBL is reasonably represented in all the resolution runs; the energy spectrum in the PBL shows the  $-5/3$  spectrum and is in good agreement with every other resolution run in the inertia subrange except the energy-dissipative range, depending on the resolution.

A dust devil is a dust-surrounded vortex, which satisfies the conditions to lift dust, i.e., large enough surface frictional velocity and suitable surface dust. However, in this study, convective vortices are examined regardless of the dust conditions in order to focus on the frequency distribution of vortices. We call the convective vortices dust devils in this paper.

We define a continuous region with a vertical vorticity greater than  $3\sigma$  as an isolated vortex and a strong vortex as one whose maximum vertical vorticity exceeds  $5\sigma$ , where  $\sigma$  is the standard deviation of the vertical vorticity in the horizontal direction. The magnitude of the threshold depends on the resolution and height. For example, the magnitude of the threshold is  $0.33 \text{ s}^{-1}$  for the 5 m resolution at 62.5 m height; the  $\sigma$  value for each resolution is shown in Table 1. The thresholds of  $3\sigma$  and  $5\sigma$  do not affect the conclusions of this study; however, the absolute number of obtained dust devils depends on the threshold. Vortex properties, such as the radius

**Table 1.** Data on Dust Devil Simulations at Different Resolutions

Resolution	100 m	50 m	25 m	10 m	5 m
Vertical level nearest 62.5 m height (m)	50	75	62.5	65	62.5
$\sigma$ at the above level at 14:30 LT ( $\text{s}^{-1}$ )	0.0087	0.017	0.032	0.066	0.11
Number of vortices at the level at 14:30 LT (density ( $\text{km}^{-2}$ ) is in brackets)	17 (0.046)	89 (0.24)	260 (0.71)	997 (2.7)	3046 (8.3)
Area fraction of vortices at the level at 14:30 LT	0.0060	0.0085	0.0098	0.0099	0.011

$R$ , maximum velocity  $U$ , pressure drop  $\Delta p$ , and circulation  $\Gamma$ , are estimated using three methods described in Text S1 in the supporting information: Rankine vortex [Rankine, 1882] fitting (RK), Burgers-Rott vortex [Burgers, 1948; Rott, 1958] fitting (BR), and maximum tangential velocity (TV) extraction. We omit vortices whose estimated  $R$  and  $U$  diverge greatly based on these three methods, since most of them have nonaxisymmetric shapes. Here the threshold for omission is a factor of 2 between the largest and smallest ones.

To determine which distribution is most likely to fit each vortex parameter, we conduct a distribution fitting (details are in Text S2). The distribution with the minimum Anderson-Darling (AD or weighted Kolmogorov-Smirnov) statistic  $D^*$  [Press et al., 2007] is assumed to be the best fit distribution. We derive the best fit distribution and its parameters from the total of six data sets independently: data sets obtained by the three vortex extraction methods at two different times (14:30 and 15:00 LT). We perform instantaneous analysis at 14:30 and 15:00 individually rather than combining the two data sets into one data set of double samples. Lorenz [2013] showed that larger vortices can survive longer than 30 min, although the average lifetime is several minutes. Thus, two different samples in a combined data set could be the same vortex. The difference of the results at two times is not large compared with the difference between the three extraction methods, and we assume them to be identically distributed samples.

### 3. Results and Discussion

Figure 1 shows the horizontal distribution of vertical velocity and vertical vorticity at 62.5 m height in the 5 m resolution run. Convective cells with hexagonal or quadrangular structures appear in the PBL, as observed in previous studies [e.g., Michaels and Rafkin, 2004]. There are strong upward motions in the narrow cell boundary and relatively weak downward motions in the entire cell region. The horizontal size of the cells is roughly 2 km at this height but tends to be smaller at lower heights. The depth of the PBL is about 6 km at this time in the runs at all resolutions.

Intense vorticity of over  $2 \text{ s}^{-1}$  is observed. The vorticity intensity depends on the experimental resolution, with more intense vorticity appearing in higher resolution runs. Intense vorticity is clearly located in the upward region; in particular, extremely intense vorticity is located near the vertices of the cells, which supports the results of previous numerical simulations [e.g., Kanak et al., 2000; Rafkin et al., 2001; Raasch and Franke, 2011].

The total number of isolated vortices depends on the altitude, with the number increasing at lower altitudes. Figure 2a shows histograms of maximum vorticity in isolated vortices in the 5 m resolution run. The horizontal axis ( $\sigma$ ) shows the standard deviation of the vorticity at each level. We choose  $\sigma$  as the horizontal axis instead of the vorticity itself to allow comparison between different levels and resolutions. The histograms produced are monotonic, and the data show a linear relationship in the log linear plot (i.e., an exponential distribution). In fact, the AD statistics show that an exponential distribution better represents the vorticity distribution than power law and lognormal distributions. The rate parameter of the exponential distribution, which corresponds to the slope of the histogram, is estimated by the method of maximum likelihood. The rate parameter depends on altitude, as shown in Figure 2b, and is steeper with height at altitudes below 50 m. A steeper distribution indicates a lower proportion of vortices with more intense vorticity. This suggests that the decreasing rate of vortices with height is greater for more intense vorticity. On the other hand, the rate parameter is almost constant above 50 m. It is about  $0.19 / \log 10$ , meaning that the frequency decreases by 1 order of magnitude per  $5\sigma$ . The decreasing rate of vortices with altitude appears to be independent of the vorticity intensity above that height.

In order to compare the histograms for different resolution runs, data at similar altitudes are used as far as possible. Some vortices are tilted, as seen in Figure 1b, and the vertical interpolation of the data can make



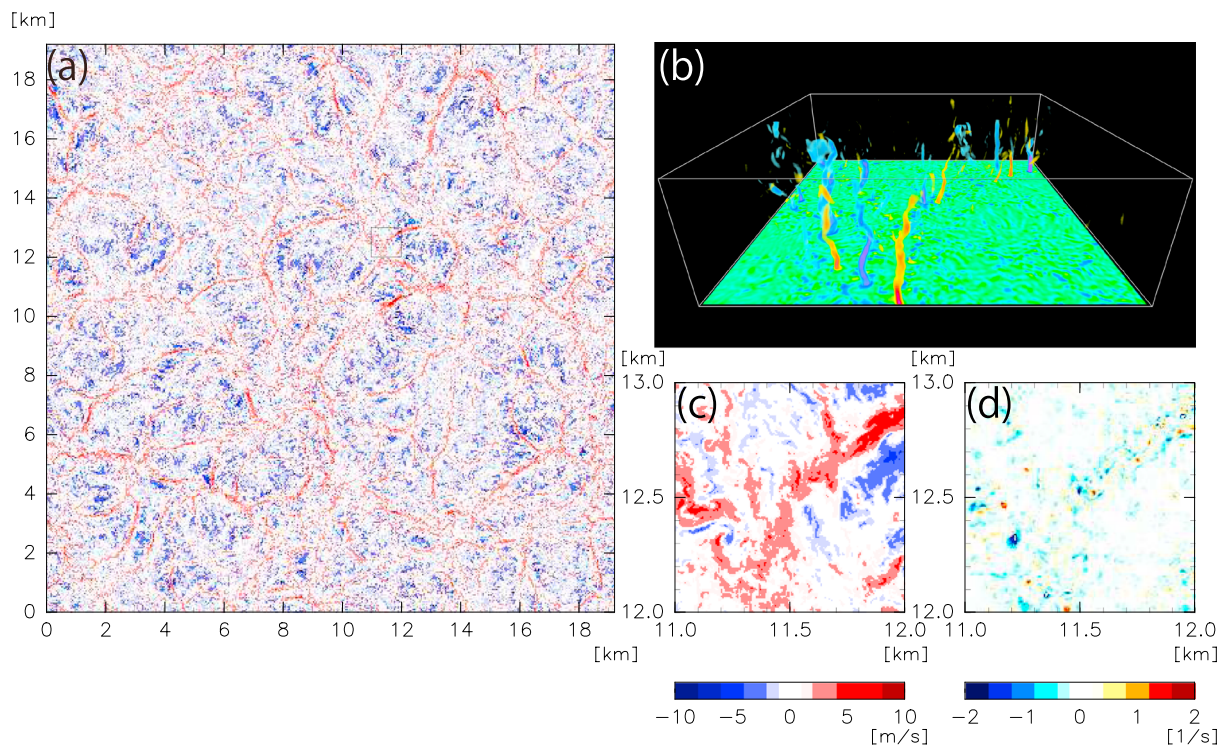


**Figure 1.** Horizontal cross sections at 62.5 m height of (a, c) vertical velocity, (d) vertical vorticity, and (b) three-dimensional structure of vertical vorticity in the 5 m resolution run at 14:30 LT. Figure 1a displays the entire domain of the simulation, while Figures 1b–1d represent the 1 km × 1 km subsection of the domain denoted by the rectangle in Figure 1a. The depth of the region in Figure 1b is 300 m from the surface. Left and right color bars correspond to vertical velocity and vertical vorticity, respectively.

deviations smaller for such tilting vortices. Therefore, we compare the data at the layer closest to 62.5 m height (Table 1) instead of using data interpolated to the same altitude. Histograms from the various resolution runs near the height of 62.5 m are shown in Figure 2c. All of the histograms produced are near monotonic, and linear relationships are observed. Deviations from the linear slope at larger intensity of vorticity seem to be due to insufficient sample numbers. The rate parameters estimated in each resolution that run higher than 25 m are almost identical, which suggests that the magnitude of the rate parameter is quantitatively robust.

The radius  $R$  and maximum horizontal velocity  $U$  of the vortices are estimated by extracting the axisymmetric vortex using the three methods (RK, BR, and TV). The number of extracted vortices is shown in Table 1. If we roughly estimate the daily number density, we obtain  $1300 \text{ km}^{-2} \text{ d}^{-1}$  for the 5 m resolution run under an assumption of an active period of 4 h and an average lifetime of 100 s, which is consistent with other terrestrial LES results [Lorenz, 2014].

Figure 3 shows histograms of the radius, maximum velocity, and pressure drop for the vortices obtained using RK. The radius histogram shows a linear relationship on the log-log plot. There are no large differences among the histograms obtained using the three methods, RK, BR, and TV, as shown in Figure S1. We perform a distribution fitting to truncated power law, exponential, and lognormal distributions, which are candidates suggested by Lorenz [2011]. Of the three distributions, a power law distribution has the smaller  $D^*$ , as shown in Table S1, and we conclude that a power law distribution is the best fit distribution for the radius. The slope of the histogram with logarithmic binning in the log-log plot corresponds to  $k + 1$ , where  $k$  is the exponent of the power law distribution. The exponent is about  $-3$  to  $-4$  for the 5 m resolution run (Table S2). It tends to be negatively larger for the coarser resolution run. The number of larger vortices tends to be larger in the coarser resolution runs. The area fraction of vortices, which is defined as  $\sum 2\pi R^2 / (19.2^2 \text{ km}^2)$ , is smaller for the coarser resolution run, despite the greater number of larger vortices in the coarser resolution run (Table 1). This suggests that small vortices are important in terms of the area of the vortices. Although there is no mode in a power law distribution, it seems natural to think that the real atmospheric vortices have a modal size due to viscosity. The mode of the histogram obtained in this study apparently depends on the resolution, even in the highest 5 m run. This suggests that the mode is smaller than 5 m.

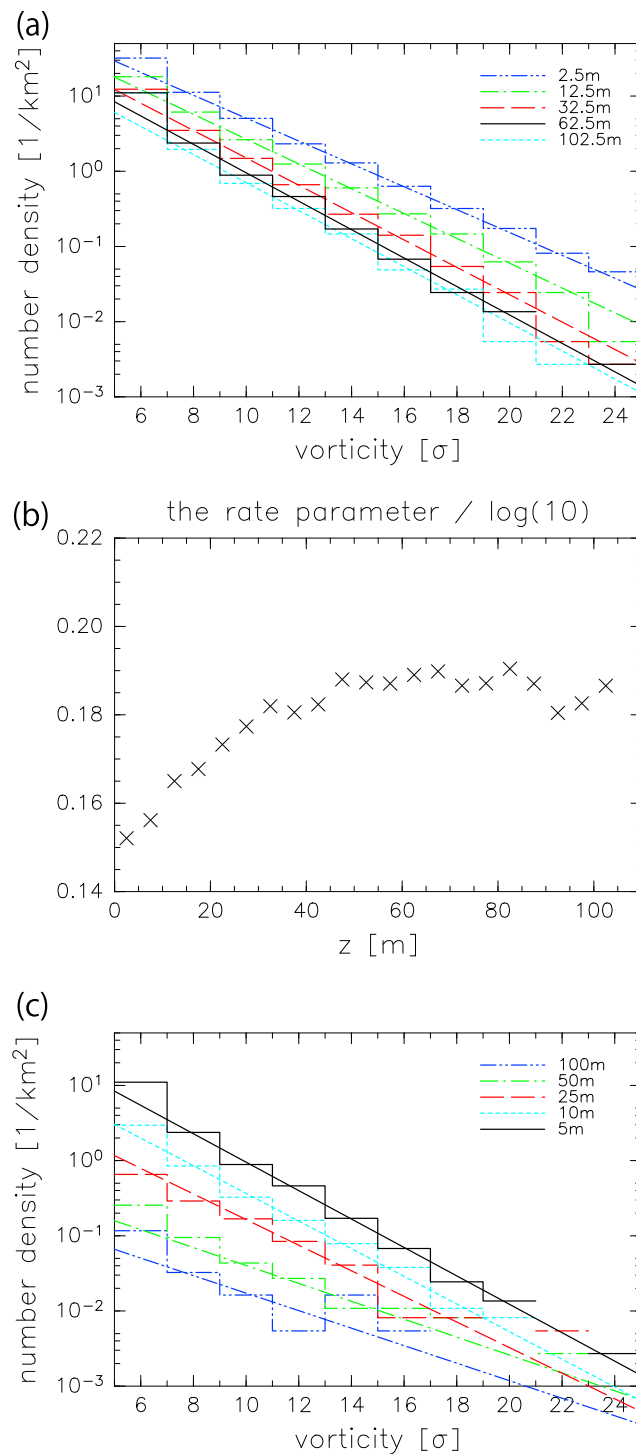


**Figure 2.** Dependency of (a) maximum vertical vorticity histograms on height in the 5 m resolution run, (b) the estimated rate parameter value of the exponential distribution of vorticity on height, and (c) maximum vertical vorticity histograms on resolution at around 62.5 m height in the 5 m resolution run. The horizontal axis in Figures 2a and 2c is normalized by the standard deviation, and colors represent altitude in Figure 2a and resolution in Figure 2c. The standard deviation is 0.0087, 0.017, 0.032, 0.066, and 0.11 s<sup>-1</sup> for the 100, 50, 25, 10, and 5 m resolution runs, respectively. The magnitude in Figure 2b is divided by log 10.

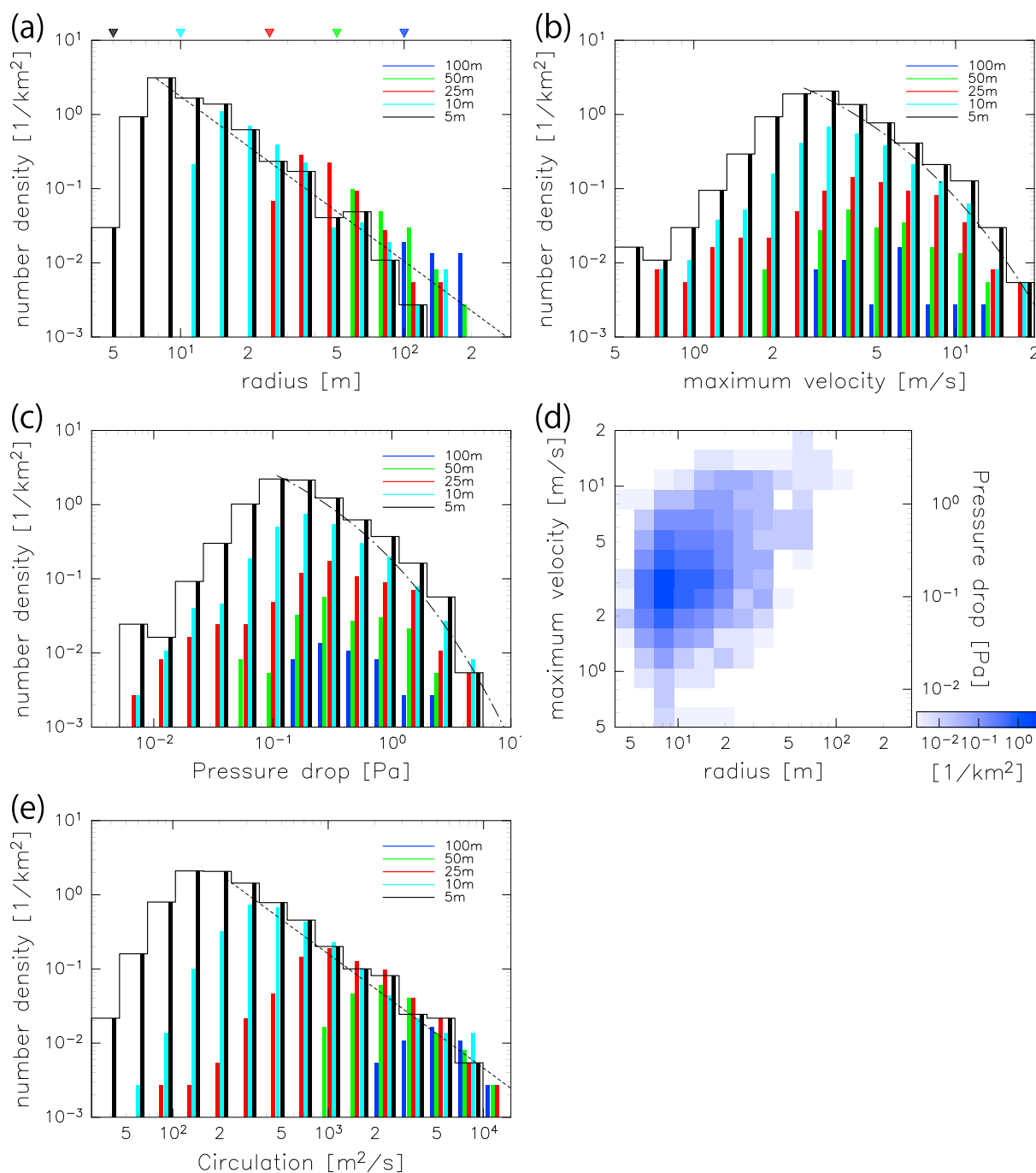


**Figure 3.** Histograms of (a) radius, (b) maximum velocity, (c) pressure drop, and (e) circulation of the vortices obtained by RK at 14:30 LT around 62.5 m height, and (d) the two-dimensional joint histogram of the radius and maximum velocity of vortices at 62.5 m height in the 5 m resolution run. In Figures 3a–3c and 3e, thin lines show the histogram of the 5 m resolution run, with the dependency of the count in each bin on the resolution shown by the bars. Colors represent resolution. The dotted line in Figures 3a and 3e represents the fitted power law distribution, and the dash-dotted line in Figures 3b and 3c represents the fitted Weibull distribution. The triangles in Figure 3a represent the grid spacing.

In contrast, the maximum velocity histogram shows neither a power law nor an exponential distribution. We additionally perform fitting to a Weibull distribution [e.g., *Fenton and Michaels, 2010*], which results in a better fit than the three other distributions in terms of the AD statistics. The shape parameter of the Weibull distribution is about 0.4–0.9 (Table S2). The mode and range of the velocity are similar for all resolution runs, with the mode being about 3–4 m/s (albeit slightly larger in the coarser resolution runs). The mode is almost independent above 20 m height, while it tends to be smaller at heights below 20 m. The maximum velocity estimated

by RK tends to be larger than that by BR and TV, as shown in Figure S1. This suggests that it is overestimated by RK, possibly because of its wedge-shaped velocity profile.

Figure 3d shows a two-dimensional joint histogram for the radius and maximum velocity. We observe a linear relationship between the radius and velocity, and the correlation coefficient between their logarithms is about 0.47. However, the data suggest that the relationship is not clear for smaller vortices. The correlation coefficient is about 0.1 for vortices with radii less than 10 m.

The pressure drop  $\Delta p$  at the center of the vortices has a histogram similar to that of the maximum velocity. It is proportional to the square of  $U$  for the Rankine and Burgers-Rott vortices. The Weibull distribution shows the best fit, as well as the maximum velocity. The mode and maximum value of the pressure drop is about 0.1 and 4.2 Pa in the 5 m resolution run. The pressure drop at the surface under the vortex center shows a similar distribution, with the mode and maximum value slightly larger than those at 62.5 m height, at about 0.3 and 4.8 Pa, respectively.

The histogram of the circulation  $\Gamma$  of the vortices is mostly linear on log-log plots, as shown in Figure 3e, and a power law is the best fit distribution. Interestingly, not only the shape but also the absolute count in the histogram bins show good agreement in each of the resolution runs. The exponent, which is about  $-2.5$  to  $-3$ , corresponding to a slope of  $-1.5$  to  $-2$  in the plot, is independent of the simulation resolution and appears to be robust.

The robustness of the distribution hints at a mechanism for determining the distribution. If a vortex merge plays an important role in intensification of vortex circulation, the merging dynamics might determine the distribution. Theoretically speaking, circulation does not change by stretching in a Lagrangian sense, while vorticity increases. This requires the existence of a vorticity source or a vortex merge in the intensification of the circulation. In general, vortices with the same sign of vorticity tend to attract each other, and vice versa, by nonlinear interactions between vortices, i.e., the beta-drift effect [e.g., *Fujiwara*, 1923; *DeMaria and Chan*, 1984; *Chan and Williams*, 1987], if their distance becomes comparable to their size. Through the merging of vortices with the same sign of vorticity, circulation is intensified. Several researchers have studied vortex merging in decaying two-dimensional turbulent flow [e.g., *McWilliams*, 1990; *Bartello and Warn*, 1996; *LaCasce*, 2008], and found that the number of vortices decays as a power law. The number decay is strongly related to the vortex merge, which suggests that the power law distribution obtained in this study might be related to the power law in the number decay in the two-dimensional turbulence case. In the PBL turbulence case, vortices are gathered into a smaller convective convergence region, and the merge could be more enhanced than in the nondivergent two-dimensional case. The relationship between vortex merge dynamics and frequency distribution presents an interesting topic for our future work.

#### 4. Concluding Remarks

The frequency distribution of dust devils is examined using a large number of samples obtained through a high-resolution and wide-domain Martian LES experiment. We sweep through spatial resolutions from 100 to 5 m in order to evaluate the robustness of the results. More than 3000 dust devils, equivalent to number density of  $8 \text{ km}^{-2}$ , are identified at 14:30 and 15:00 LT in the 5 m resolution run, allowing a robust statistical analysis of their histograms. The maximum vertical vorticity of the dust devils has an exponential distribution, with a rate parameter of 10 per  $5\sigma$  above 50 m height, where  $\sigma$  is the standard deviation of magnitude of vorticity. The distribution type and distribution parameter are robust in the sense that they are independent of resolution. The radius and maximum velocity of the dust devils are estimated using three methods at 14:30 and 15:00 LT. Our results strongly support a power law distribution; the distribution type of dust devil radius has been considered in previous studies, and several distributions have been proposed. The exponent of the power law distribution depends on the resolution. It ranges from  $-3$  to  $-4$  for the 5 m resolution run and is more negative for the coarser resolution run. The maximum velocity has a mode of 3–4 m/s, which is marginally smaller in higher resolution runs. The maximum pressure drop is about 4.2 Pa in the 5 m resolution run. Histograms of the maximum velocity and pressure drop have similar shapes, and they appear to have a Weibull distribution.

We find that vortex circulation has a power law distribution with an exponent in the range of  $-2.5$  to  $-3$ . We speculate that this distribution is determined by the dynamics of vortex merging. If intensification of vortex



circulation is dominated by a vortex merge, the representation of weak vortices affects that of strong vortices in a simulation, which implies that resolution may affect even large dust devils in simulations.

Knowledge and understanding of the frequency distributions of dust devils can improve representations of dust injection in large-scale numerical simulations of the Martian atmosphere. In Martian general circulation and mesoscale models, there exist two types of parameterizations: dust lifting by large-scale wind stress, represented by the Monin-Obukov similarity theory (wind stress parameterization), and small-scale convective motion (convective parameterization) [e.g., Newman *et al.*, 2002; Basu *et al.*, 2004; Kahre *et al.*, 2006]. The effect of dust devils is taken into account in convective parameterization; however, in this approach, the effect is implicitly estimated based on the heat engine theorem [Rennó *et al.*, 1998] but not explicitly estimated from dust devil statistics. Our results represent the first step in the development of a more sophisticated parameterization based on the frequency distribution of dust devils.

## Acknowledgments

The authors would like to thank the Editor and the two referees, Spiga and Lorenz, for fruitful discussions. This research used the computational resources (K computers) of the RIKEN Advanced Institute for Computational Science through the HPCI System Research project (Project ID: hp120076 and hp140171). Figures in the manuscript were created using the products of the GFD-Dennou Club (<http://www.gfd-dennou.org/>) and VAPOR (<http://www.vapor.ucar.edu/>). Data for this paper are available from the authors upon request ([s-nishizawa@riken.jp](mailto:s-nishizawa@riken.jp)).

## References

- Barcello, P., and T. Warn (1996), Self-similarity of decaying two-dimensional turbulence, *J. Fluid Mech.*, **326**, 357–372.
- Basu, S., M. I. Richardson, and R. J. Wilson (2004), Simulation of the Martian dust cycle with the GFDL Mars GCM, *J. Geophys. Res.*, **109**, E11006, doi:10.1029/2004JE002243.
- Brown, A. R., S. H. Derbyshire, and P. J. Mason (1994), Large-eddy simulation of stable atmospheric boundary layers with a revised stochastic subgrid model, *Q. J. R. Meteorol. Soc.*, **120**, 1485–1512.
- Burgers, J. M. (1948), A mathematical model illustrating the theory of turbulence, *Adv. Appl. Mech.*, **1**, 171–199.
- Cantor, B. A., P. B. James, M. Caplinger, and M. J. Wolff (2001), Martian dust storms: 1999 Mars Orbiter Camera observations, *J. Geophys. Res.*, **106**, 23,653–23,687, doi:10.1029/2000JE001310.
- Chan, J. C. L., and R. T. Williams (1987), Analytical and numerical studies of the beta-effect in tropical cyclone motion. Part I: Zero mean flow, *J. Atmos. Sci.*, **44**, 1257–1265.
- DeMaria, M., and J. C. L. Chan (1984), Comments on “A numerical study of the interactions between two tropical cyclones”, *Mon. Weather Rev.*, **112**, 1643–1645.
- Fenton, L. K., and R. Lorenz (2015), Dust devil height and spacing with relation to the Martian planetary boundary layer thickness, *Icarus*, **260**, 246–262.
- Fenton, L. K., and T. I. Michaels (2010), Characterizing the sensitivity of daytime turbulent activity on Mars with the MRAMS LES: Early results, *Mars*, **5**, 159–171, doi:10.1555/mars.2010.0007.
- Fujiwara, S. (1923), On the growth and decay of vortical systems, *Q. J. R. Meteorol. Soc.*, **49**, 75–104.
- Gheynani, B. T., and P. A. Taylor (2011), Large eddy simulation of typical dust devil-like vortices in highly convective Martian boundary layers at the Phoenix lander site, *Planet. Space Sci.*, **59**, 43–50, doi:10.1016/j.pss.2010.10.011.
- Greeley, R., A. Skyeck, and J. B. Pollack (1993), Martian aeolian features and deposits: Comparisons with general circulation model results, *J. Geophys. Res.*, **98**, 3183–3196, doi:10.1029/92JE02580.
- Hinson, D. P., M. Pätzold, S. Tellmann, B. Häusler, and G. L. Tyler (2008), The depth of the convective boundary layer on Mars, *Icarus*, **198**, 57–66.
- Iversen, J. D., and B. R. White (1982), Saltation threshold on Earth, Mars and Venus, *Sedimentology*, **29**, 111–119, doi:10.1111/j.1365-3091.1982.tb01713.x.
- Kahre, M. A., J. R. Murphy, and R. M. Haberle (2006), Modeling the Martian dust cycle and surface dust reservoirs with the NASA Ames general circulation model, *J. Geophys. Res.*, **111**, E06008, doi:10.1029/2005JE002588.
- Kanak, K. M., D. K. Lilly, and J. T. Snow (2000), The formation of vertical vortices in the convective boundary layer, *Q. J. R. Meteorol. Soc.*, **126**, 2789–2810.
- LaCasce, J. H. (2008), The vortex merger rate in freely decaying, two-dimensional turbulence, *Phys. Fluids*, **20**, 85102, doi:10.1063/1.2957020.
- Lemmon, M. T., et al. (2004), Atmospheric imaging results from the Mars Exploration Rovers: Spirit and opportunity, *Science*, **306**, 1753–1756.
- Lorenz, R. (2011), On the statistical distribution of dust devil diameters, *Icarus*, **215**, 381–390.
- Lorenz, R. (2013), The longevity and aspect ratio of dust devils: Effects on detection efficiencies and comparison of landed and orbital imaging at Mars, *Icarus*, **226**, 964–970, doi:10.1016/j.icarus.2013.06.031.
- Lorenz, R. D. (2014), Vortex encounter rates with fixed barometer stations: Comparison with visual dust devil counts and large-eddy simulations, *J. Atmos. Sci.*, **71**, 4461–4472, doi:10.1175/JAS-D-14-0138.1.
- Louis, J.-F. (1979), A parametric model of vertical eddy fluxes in the atmosphere, *Boundary Layer Meteorol.*, **17**, 187–202.
- McWilliams, J. C. (1990), The vortices of two-dimensional turbulence, *J. Fluid Mech.*, **219**, 361–385.
- Michaels, T. I., and S. C. R. Rafkin (2004), Large-eddy simulation of atmospheric convection on Mars, *Q. J. R. Meteorol. Soc.*, **130**, 1251–1274, doi:10.1256/qj.02.169.
- Newman, C. E., S. R. Lewis, and P. L. Read (2002), Modeling the Martian dust cycle 1. Representations of dust transport processes, *J. Geophys. Res.*, **107**(E12), 5123, doi:10.1029/2002JE001910.
- Nishizawa, S., H. Yashiro, Y. Sato, Y. Miyamoto, and H. Tomita (2015), Influence of grid aspect ratio on planetary boundary layer turbulence in large-eddy simulations, *Geosci. Model Dev.*, **8**, 3393–3419, doi:10.5194/gmd-8-3393-2015.
- Odaka, M. (2001), A numerical simulation of Martian atmospheric convection with a two-dimensional anelastic model: A case of dust-free Mars, *Geophys. Res. Lett.*, **28**, 895–898, doi:10.1029/2000GL012090.
- Odaka, M., K. Nakajima, M. Ishiwatari, and Y.-Y. Hayashi (2001), A numerical simulation of thermal convection in the Martian lower atmosphere with a two-dimensional anelastic model, *Nagare Multimedia*. [Available at <http://www2.nagare.or.jp/mm/2001/odaka/index.htm>.]
- Ohno, H., and T. Takemi (2010), Mechanisms for intensification and maintenance of numerically simulated dust devils, *Atmos. Sci. Lett.*, **11**, 27–32, doi:10.1002/asl.249.
- Petrosyan, A., et al. (2011), The Martian atmospheric boundary layer, *Rev. Geophys.*, **49**, RG3005, doi:10.1029/2010RG000351.
- Press, W. H., S. A. Teukolsky, W. T. Vetterling, and B. P. Flannery (2007), *Numerical Recipes in C: The Art of Scientific Computing*, 3rd ed., Cambridge Univ. Press, New York.

- Raasch, S., and T. Franke (2011), Structure and formation of dust devil-like vortices in the atmospheric boundary layer: A high-resolution numerical study, *J. Geophys. Res.*, **116**, D16120, doi:10.1029/2011JD016010.
- Rafkin, S. C. R., R. M. Haberle, and T. I. Michaels (2001), The Mars regional atmospheric modeling system: Model description and selected simulations, *Icarus*, **151**, 228–256.
- Rafkin, S. C. R., J. L. Hollingsworth, M. A. Mischna, C. E. Newman, and M. I. Richardson (2013), Mars: Atmosphere and climate overview, in *Comparative Climatology of Terrestrial Planets*, edited by S. J. Mackwell et al., pp. 55–89, Univ. of Arizona Press, Tucson, Tex.
- Rankine, W. J. M. (1882), *A Manual of Applied Physics*, 10th ed., 663 pp., Charles Griff and Co., London.
- Rennó, N. O., M. L. Burkett, and M. P. Larkin (1998), A simple thermodynamical theory for dust devils, *J. Atmos. Sci.*, **55**, 3244–3252.
- Rott, N. (1958), On the viscous core of a line vortex, *Z. Math. Phys.*, **9b**, 543–553.
- Sato, Y., S. Nishizawa, H. Yashiro, Y. Miyamoto, Y. Kajikawa, and H. Tomita (2015), Impacts of cloud microphysics on trade wind cumulus: Which cloud microphysics processes contribute to the diversity in a large eddy simulation?, *Prog. Earth Planet. Sci.*, **2**, 23, doi:10.1186/s40645-015-0053-6.
- Scotti, A., C. Meneveau, and D. K. Lilly (1993), Generalized Smagorinsky model for anisotropic grids, *Phys. Fluids A-Fluid*, **5**, 2306–2308.
- Thomas, P., and P. J. Gierasch (1985), Dust devils on Mars, *Science*, **230**, 175–177.
- Toigo, A. D., M. I. Richardson, S. P. Ewald, and P. J. Gierasch (2003), Numerical simulation of Martian dust devils, *J. Geophys. Res.*, **108**, 5047, doi:10.1029/2002JE002002.
- Uno, I., X.-M. Cai, D. G. Steyn, and S. Emori (1995), A simple extension of the Louis method for rough surface layer modeling, *Boundary Layer Meteorol.*, **76**, 395–409.
- Wilson, R. J., and K. Hamilton (1996), Comprehensive model simulation of thermal tides in the Martian atmosphere, *J. Atmos. Sci.*, **53**, 1290–1326.